AMERICAN SOCIETY of
GENE & CELL
THERAPY

Improving T Cell Receptor On-Target Specificity via Structure-Guided Design

Lance M. Hellman,[1,4] Kendra C. Foley,[2,4] Nishant K. Singh,[1] Jesus A. Alonso,[1] Timothy P. Riley,[1] Jason R. Devlin,[1] Cory M. Ayres,[1] Grant L.J. Keller,[1] Yuting Zhang,[1] Craig W. Vander Kooi,[3] Michael I. Nishimura,[2] and Brian M. Baker[1]

[1]Department of Chemistry and Biochemistry and the Harper Cancer Research Institute, University of Notre Dame, Notre Dame, IN, USA; [2]Department of Surgery and the Cardinal Bernardin Cancer Center, Loyola University of Chicago, Maywood, IL, USA; [3]Department of Molecular and Cellular Biochemistry, University of Kentucky, Lexington, KY, USA

T cell receptors (TCRs) have emerged as a new class of immunological therapeutics. However, though antigen specificity is a hallmark of adaptive immunity, TCRs themselves do not possess the high specificity of monoclonal antibodies. Although a necessary function of T cell biology, the resulting cross-reactivity presents a significant challenge for TCR-based therapeutic development, as it creates the potential for off-target recognition and immune toxicity. Efforts to enhance TCR specificity by mimicking the antibody maturation process and enhancing affinity can inadvertently exacerbate TCR cross-reactivity. Here we demonstrate this concern by showing that even peptide-targeted mutations in the TCR can introduce new reactivities against peptides that bear similarity to the original target. To counteract this, we explored a novel structure-guided approach for enhancing TCR specificity independent of affinity. Tested with the MART-1-specific TCR DMF5, our approach had a small but discernible impact on cross-reactivity toward MART-1 homologs yet was able to eliminate DMF5 cross-recognition of more divergent, unrelated epitopes. Our study provides a proof of principle for the use of advanced structure-guided design techniques for improving TCR specificity, and it suggests new ways forward for enhancing TCRs for therapeutic use.

INTRODUCTION

T cells orchestrate cellular immunity through their clonotypic T cell receptors (TCRs), which recognize peptide antigens bound and presented by major histocompatibility complex (MHC) proteins. TCRs have emerged as a new class of immunological therapeutics, most prominently for cancer, where clinical trials with T cells redirected toward tumor antigens with exogenous TCR genes have shown that objective clinical responses can be obtained for patients with advanced malignancies.[1–6] Similar approaches are in development for the treatment of infectious diseases, such as tuberculosis, HIV, and hepatitis C virus (HCV).[7–9] However, adverse events have occurred in some trials with gene-modified T cells, attributable in some cases to TCR recognition of off-target epitopes. In one striking example, a TCR targeting the MAGE-A3 melanoma antigen cross-reacted with an antigen from the muscle protein Titin, leading to cardiovascular toxicity and deaths.[10]

TCR cross-reactivity, sometimes referred to as polyspecificity,[11] is a fundamental aspect of cellular immunity, as it permits the fixed-size TCR repertoire to engage a much larger universe of potential antigens.[12,13] Although TCR cross-reactivity is a biological necessity, the capacity to recognize multiple antigens presents a significant challenge for the development of TCR-based immunotherapies. Approaches to further understand and potentially improve receptor specificity are thus now of critical import. Building on lessons learned from antibody maturation, affinity-enhanced TCRs might be expected to yield enhanced specificity. Unlike antibodies though, large gains in TCR affinity can in fact lead to increased cross-reactivity (although see Gee et al.[14] for an exception).[15–17] One reason for this is the structural organization of the TCR ligand: in most peptide/MHC complexes, the small amount of exposed surface area of the peptide compared to the MHC protein limits the number of peptide-specific features against which any one TCR can be optimized. Thus, mutations that enhance TCR affinity can also enhance it for multiple peptides, or worse, they can indiscriminately enhance affinity by improving interactions between TCR and MHC protein without regard to peptide.[18]

In addition to improving TCR specificity, enhancing TCR affinity has also been explored as a strategy to improve T cell potency toward specific antigens.[19–21] Indeed, studies show increased potency with gains in affinity up to a point.[15,22–27] However, very high, supraphysiological TCR affinities can lead to impaired T cell function.[17,28–30] Thus, in light of the impact of affinity on specificity and function, multiple authors have suggested that optimal TCR affinity may lie within the range characteristic of strong anti-viral immune responses, i.e., a binding affinity (or K_D) in the low micromolar range.[18–21,31]


Table 1. Cross-Reactivity Panel Based on Previously Identified Peptides Reactive with MART-1-Specific TCRs

Peptide	Sequence
MART-1 [9-mer]	AAGIGILTV
MART-1 [10-mer]	ELAGIGILTV
M. tuberculosis protein 2 (Mtub2)	IAGPGTITL
Human CD9 (hCD9)	AVGIGIAVV
HSV-2 glycoprotein F (HSV-2 gpF)	GAGIGVAVL
β-endoxylanase	GAGIGVLTA
Human elongation factor 1α (hEF1α)	IGGIGTVPV
G-protein coupled receptor (GPCR)	ALGLGLLPV
Human receptor expression enhancing I (hREP1)	LGVIGLVAL
HSV-1 glycoprotein 3 (HSV-1 gp3)	IAGIGILAI
ADP-ribose diphosphatase (ADP)	VDGIGILTI
ImrA	LAGIGLIAA
M. tuberculosis protein 1 (Mtub1)	LGGLGLFFA

As a step toward developing novel ways to enhance TCR specificity, we recently utilized a structure-guided design approach to generate variants of the DMF5 TCR, which recognizes the MART-1 melanoma antigen presented by the class I MHC protein HLA-A*0201 (HLA-A2).[32,33] Unlike molecular evolution approaches, such as yeast or phage display, structure-guided design can, in principle, be used to target peptide-specific features. Our design approach yielded variants with a range of affinity enhancement, with the strongest possessing nanomolar affinity toward the MART-1 decamer, approximately 400-fold greater than wild-type.

In this study, we explored how our structure-guided design efforts impacted the specificity of the DMF5 TCR. We found that enhancing TCR affinity did indeed introduce greater cross-reactivity toward other epitopes sharing the MART-1 core sequence, highlighting the danger that exists even with peptide-targeted affinity enhancing mutations. We then asked whether a structure-guided design approach that incorporated the principles of both positive and negative designs could fine-tune receptor binding in a way that reduces cross-reactivity yet maintains affinity near optimal levels. Approaches combining positive and negative designs have been used in other fields to optimize binding specificity, and they involve the simultaneous use of affinity-enhancing and affinity-weakening mutations in different regions of the interface.[34] Our implementation had a small but discernible impact on DMF5 cross-recognition of MART-1 homologs. We were, however, able to eliminate cross-recognition of other more divergent cross-reactive epitopes while still retaining reactivity toward MART-1. Although further testing and development is needed, our results provide a proof of principle for the combined use of structure-guided positive and negative designs in rationally manipulating TCR specificity and suggest new strategies for creating enhanced TCRs safer for therapeutic use.
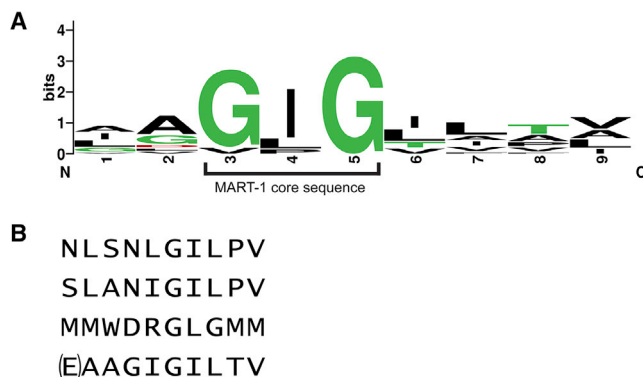
Figure 1. MART-1 Homologs and More Diverse Epitopes Recognized by the DMF5 TCR

(A) Sequence logo of the previously identified nonameric MART-1 homologs shown in Table 1 that cross-react with MART-1-specific TCRs.[36] The GIG sequence spanning positions 3–5, referred to as the MART-1 core sequence, is highlighted. The logo excludes the N-terminally extended MART-1 decamer. The logo was created using WebLogo.[76] (B) Divergent epitopes also recognized by DMF5. The top peptide is the NLS epitope, identified via yeast display screening. The second peptide is the SLA epitope, identified via structural modeling. The third peptide is the MMW epitope, also identified through yeast display. The bottom peptide shows the native MART-1 decamer for reference, with the p1 glutamate in parentheses, as DMF5 and most MART-1 TCRs studied recognize both nonameric and decameric MART-1, including p2 anchor-modified variants as studied here.

RESULTS

High-Affinity DMF5 Variants Show Enhanced Recognition of MART-1 Homologs

We previously used structure-guided computational design to engineer variants of the DMF5 TCR that bound the MART-1 anchor-modified decamer (ELAGIGILTV) presented by HLA-A2 with stepwise improvements in binding affinity, with K_D values ranging from the low micromolar to low nanomolar.[32,35] The mutations that imparted high affinity were engineered with an emphasis on the TCR-peptide interaction, utilizing the crystal structure of DMF5 bound to the MART-1 decamer presented by HLA-A2 for structure-guided computational design.[32]

To ask how enhancing affinity toward MART-1/HLA-A2 influenced TCR cross-reactivity, we surveyed the reactivity of the DMF5 TCR and its high-affinity variants (L98βW, D26αY, and the D26αY/L98βW double mutant, referred to as DMF5$_{YW}$) against a panel of peptides previously shown to be recognized by many MART-1-reactive T cells (Table 1).[36] This panel includes peptides of both human and pathogen origin, as well as the native MART-1 nonamer. The peptide panel is characterized by a strongly conserved glycine-isoleucine-glycine central core sequence, although the individual peptides differ near the N and C termini (Figure 1A).

Reactivity toward the peptide panel was assessed via intracellular interferon (IFN)-γ production by co-culturing TCR-transduced T cells with peptide-pulsed antigen-presenting cells (Figure 2A). As
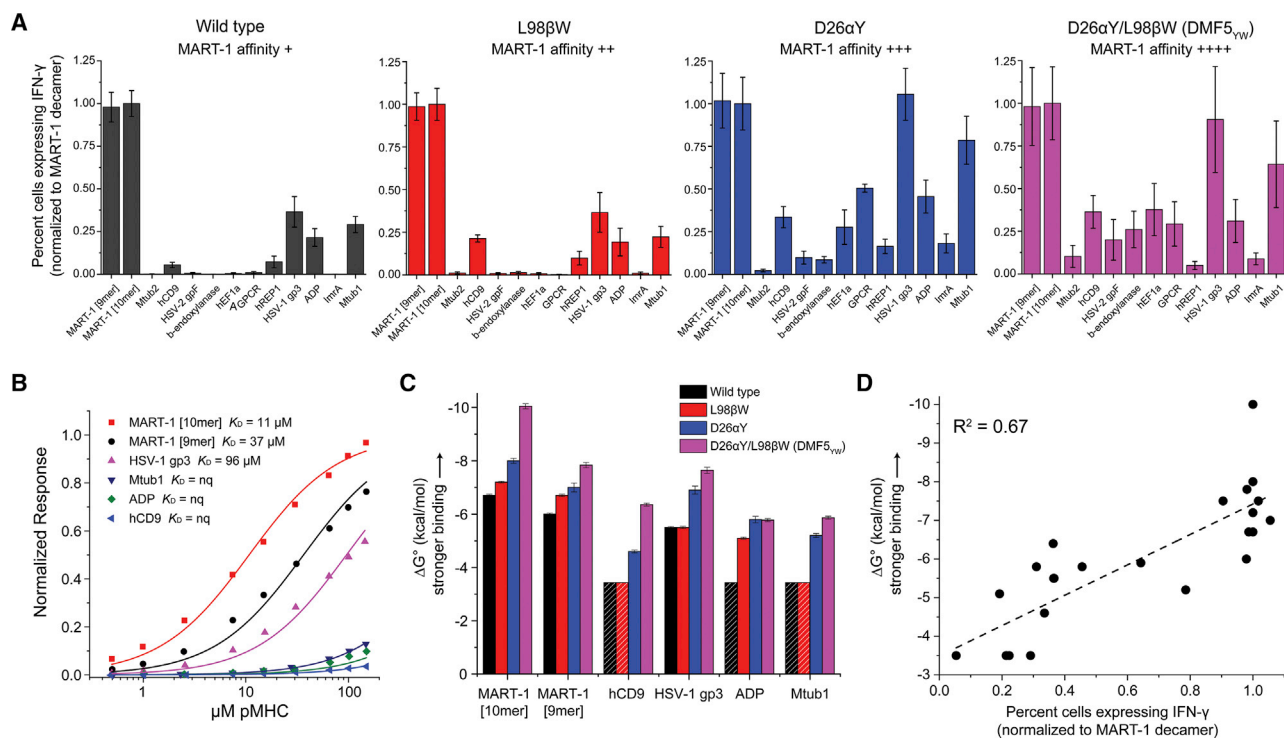
Figure 2. Enhancing TCR Affinity toward MART-1 Leads to Increased Cross-Reactivity and Ultimately Decreased T Cell Potency

(A) Percent transduced CD8^{+} T cells expressing intracellular IFN-γ after co-culturing TCR-transduced PBMCs with T2 cells pulsed with the MART-1 peptides and each of the MART-1 homologs in Table 1. As affinity toward MART-1 nonamer or decamer is enhanced, as indicated in the insets, TCR cross-reactivity increases. Data are averages of six sets of experiments (two independent repeats from three donors), normalized to the values for the MART-1 decamer. Error bars indicate SEM. (B) Wild-type DMF5 binds MART-1 homologs weaker than it does the MART-1 nonamer or decamer, as measured by surface plasmon resonance. nq, binding detectable, but too weak to quantify. (C) Strengthening affinity toward MART-1 nonamer or decamer strengthens affinity toward the homologs, as shown by the increase in favorable binding free energy. Shaded bars represent minimum ΔG° estimates where binding was detectable but too weak to quantify. Error bars represent fitting errors from global fitting of multiple datasets, as described in the Materials and Methods, propagated from errors in K_D. (D) For those complexes that could be generated recombinantly, functional responses from (A) correlate well with binding free energies from (C).

the DMF5 variants showed slightly different stabilities (Figure S1) and in order to compare relative reactivities, data for each TCR were normalized to the values for the MART-1 decamer. T cells transduced with wild-type DMF5 strongly recognized the MART-1 peptides, although the wild-type receptor weakly recognized several other peptides in the panel. The L98βW mutation, which results in a ∼2-fold enhancement in DMF5-binding affinity toward the MART-1 decamer,[32] had little impact on cross-recognition. However, the D26αY mutation, which has a more substantial ∼10-fold enhancement on the binding of DMF5 to the MART-1 decamer, had a more significant impact on cross-reactivity. The D26αY mutant recognized additional peptides not recognized by the wild-type TCR, and peptides that were recognized weakly by the wild-type receptor were recognized as strongly as MART-1. This pattern of broader cross-recognition was maintained by the highest affinity DMF5_YW double mutant (∼400-fold enhancement over wild-type).

The functional experiments indicate that enhancing the affinity of the DMF5 TCR toward the target or cognate MART-1 decamer increased the likelihood that the TCR would cross-react with other peptides

similar to MART-1. To relate these observations to physical properties, we measured the binding of the wild-type and higher affinity DMF5 TCR variants to various peptide/MHC complexes (pMHCs) from the cross-reactivity panel in Table 1. Although we were unable to generate stable recombinant pMHCs for the entire panel, we were able to produce protein and perform measurements with the human CD9 (hCD9), HSV-1 glycoprotein 3 (HSV-1 gp3), ADP-ribose diphosphatase, and *M. tuberculosis* protein 1 (Mtub1) peptides. Thermal stability measurements indicated that the affinity of each peptide to HLA-A2 was intermediate between that of the MART-1 nonamer and anchor-modified decamer (Figure S1), confirming the production of stable pMHCs and indicating that differing functional results with this set of peptides are unlikely to be attributable to variations in peptide binding to HLA-A2.

Binding experiments using surface plasmon resonance (SPR) revealed that the binding of wild-type DMF5 to each of the off-target complexes was indeed weaker than binding to complexes with either the MART-1 nonamer or decamer (Figure 2B). Binding was detected in all cases, but, despite using an SPR approach that utilizes global
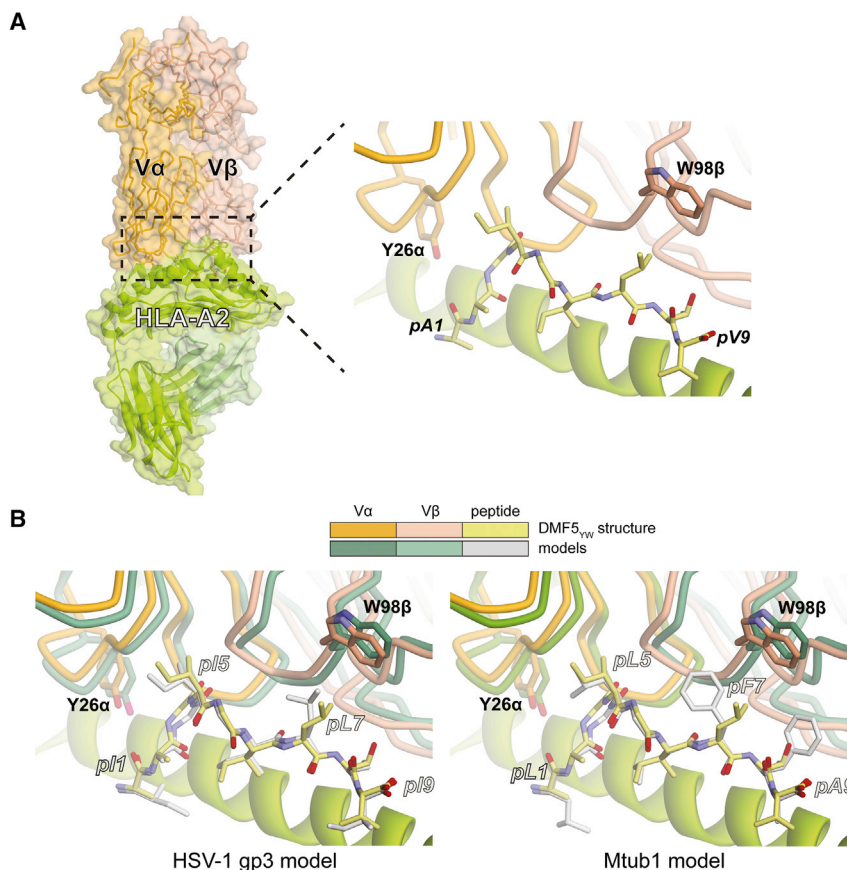
Figure 3. Structural Basis for the Lack of Selectivity with the High-Affinity DMF5 Mutations toward MART-1 Homologs

(A) Interface between the high-affinity DMF5$_{YW}$ variant and the MART-1 nonamer presented by HLA-A2, as revealed by the crystallographic structure of the complex. (B) Modeling of the HSV-1 gp3 and Mtub1 peptides in the interface DMF5$_{YW}$ forms with the MART-1 nonamer presented by HLA-A2 interface suggests there are no requirements for significant conformational changes and that the environments around the high-affinity mutations are conserved.

enhanced TCR-peptide packing along the C-terminal half of the peptide. However, despite being designed using structural data with the MART-1 decamer and targeting peptide regions outside the conserved core sequence, our data indicate that the effects of the affinity-enhancing mutations were not highly specific for the MART-1 nonamer or decamer.

To understand how the mutations that conferred high affinity toward MART-1 sequences also permitted enhanced recognition of the other peptides, we examined structural properties within the TCR-pMHC interfaces. To better compare with the cross-reactive nonameric peptides shown in Figure 1A and Table 1, we first crystallized and determined the X-ray structure of the highest affinity DMF5$_{YW}$ double mutant with the MART-1 nonamer presented by HLA-A2 (Figure 3A; Table S2). Clear electron density was present throughout the TCR-peptide/MHC interface (Figure S2). Except for the lack of the p1 glutamate, the nonameric structure is essentially identical to the previously determined structure with the decamer (all common TCR-pMHC atoms superimpose with a root-mean-square deviation [RMSD] of 1.6 Å).[32] The nonameric peptide adopts the same conformation as the decamer (all common peptide atoms superimpose with an RMSD of 0.3 Å). Lacking the N-terminal glutamate, the HLA-A2 A pocket is empty, and the peptide p1 alanine occupies the HLA-A2 B pocket (i.e., the alanine at peptide position 1 serves as the first primary anchor). The complementarity determining region (CDR) loops of the TCR are in the same positions as in the decameric structure, as are the side chains of Tyr26α and Trp98β.

fitting of multiple datasets to enhance sensitivity and accuracy,[37,38] binding to some peptides was at or near our limit for quantification. However, TCR affinity toward each of the peptides was strengthened as affinity toward the MART-1 epitopes was increased. This is most easily demonstrated by comparing binding free energy changes (ΔG° values), as shown in Figure 2C (full quantification in Table S1). Thus, enhancing affinity of DMF5 toward MART-1 also enhanced affinity toward other MART-1 homologs with similar core sequences. The enhancement in binding affinity correlated well with the stronger functional responses (Figure 2D). This result highlights a risk of adopting affinity-enhanced TCRs for therapeutic use: even if the mutations that confer high affinity are designed to target the cognate peptide, reactivities towards similar peptides are likely to be introduced.

Structural Basis for the Lack of Selectivity with High-Affinity Mutations

As noted above, the two mutations that imparted high affinity to the DMF5 TCR toward MART-1/HLA-A2 were engineered with an emphasis on the TCR-peptide interaction, utilizing structural information. The crystal structure of the high-affinity TCR-pMHC indicated that the D26αY mutation eliminated the aspartate's desolvation penalty and led to better packing near the peptide N terminus by burying additional hydrophobic surface.[32] The L98βW mutation

We next used the DMF5$_{YW}$ structure with the MART-1 nonamer to model recognition of the HSV-1 gp3 and Mtub1 peptides, the two most strongly recognized in the cross-reactivity screen in Figure 2A. Rather than attempting to capture the fine structural details of these complexes, our goal was to ask if the two peptides could fit into the DMF5$_{YW}$ complex without necessitating large structural shifts. Using a relaxed structure with the nonameric MART-1 peptide as a template, we substituted the peptide side chains and repacked the interface using the Rosetta protein design suite to optimize geometry,

interatomic interactions, and eliminate clashes.[39] As shown in Figure 3B, modeling indicated that the sequence differences between HSV-1 gp3 and Mtub1 peptides did not necessitate any significant rearrangements: both peptides could be threaded into the DMF5$_{YW}$-MART-1/HLA-A2 structure without requiring substantial changes in the TCR CDR loops or their side chains. Furthermore, the environments around the mutation sites are conserved between complexes, i.e., the geometries are similar and there are no significant changes in interface chemistry.

Overall, these results indicate that the physicochemical mechanisms underlying the stronger affinity of the DMF5$_{YW}$ double mutant toward the MART-1 nonamer and decamer are maintained with the other peptides in Table 1. In the case of the D26αY mutation, since the amino acids at position p1 occupy the HLA-A2 B pocket and because p2 in all but one case is a small side chain that points away from the TCR, the tyrosine is unable to differentiate between sequence and structural differences among the various peptides. In the case of the L98βW mutation, the closest MART-1 amino acid is the leucine at position 7. In all cases, the p7 positions in the peptides are hydrophobic amino acids (Figure 1A), and again the tryptophan seems unable to differentiate between the differences. Additionally, we cannot rule out the possibility that, due to the close proximity of the peptide and the HLA-A2 α1 and α2 helices, the D26αY and L98βW mutations strengthen interactions with the MHC protein, which could also contribute to the inability of the high-affinity DMF5$_{YW}$ variant to distinguish between related peptides.

Cross-Recognition of Alternative Epitopes by the Wild-Type DMF5 TCR and High-Affinity Variant

Our data thus far indicate that the structure-guided mutations in DMF5 that enhanced affinity toward MART-1 also enhanced affinity toward MART-1 homologs, increasing cross-reactivity. Importantly though, many peptides cross-reactive with any given TCR will not share high sequence homology.[40,41] We thus examined DMF5 recognition of peptides not identified via a MART-1 homology search (Figure 1B). We first selected a decameric peptide identified in a yeast display screen of the wild-type DMF5 TCR termed MMW (sequence MMWDRGLGMM).[42] We previously showed that recognition of MMW by DMF5 requires complex architectural changes in both the peptide and the HLA-A2 protein.[43] These occur in part because of the bulky tryptophan at p3 and the suboptimal methionine at the p10 anchor, which result in the peptide shifting its register upon TCR binding such that the C terminus extends from the HLA-A2-binding groove.

As with the MART-1 homologs, the D26αY and L98βW mutations in DMF5$_{YW}$ resulted in stronger, nanomolar-binding affinity toward MMW, with a ΔΔG° of −3.5 kcal/mol, close to the value of −3.2 kcal/mol observed with the MART-1 decamer (Table S1). Superimposing the TCR from the DMF5$_{YW}$ complex onto wild-type DMF5 in the complex with MMW indicated the two high-affinity mutations could be accommodated without significant structural alterations, just as seen with the MART-1 homologs as shown in Figure 3.

We next examined two other peptides that diverge from both MART-1 and MMW. These peptides, termed NLS (sequence NLSNLGILPV) and SLA (sequence SLANIGILPV), differ primarily from MART-1 and other peptides in the homology panel through the presence of asparagine at position p4, whereas all but one of the MART-1 peptides and homologs retain a glycine at the equivalent position (Figure 1A). In direct binding experiments, NLS and SLA were recognized by wild-type DMF5 with micromolar affinities close to wild-type DMF5 recognition of the MART-1 decamer (Figure 4A; Table S1). Surprisingly, however, unlike the MART-1 homologs and the MMW peptide, binding affinities toward NLS and SLA were largely unchanged with the DMF5$_{YW}$ variant (i.e., the mutations that confer high affinity toward the MART-1 homologs and MMW do not do so with the NLS and SLA peptides). Modeling indicated that this could be attributable at least in part to the p4 asparagine, which while tolerated by wild-type DMF5, with DMF5$_{YW}$ is predicted to insert into a more tightly packed electrostatic environment, displacing an interfacial water molecule and altering the position of Gln30 of CDR1α. Together these offset the affinity enhancements from the D26αY and L98βW mutations (Figure 4B). Thus, NLS and SLA are recognized with very similar, low micromolar affinities by both wild-type and high-affinity DMF5$_{YW}$.

Implementation of a Positive and Negative Design Strategy to Focus TCR Specificity

We next asked if we could more rationally manipulate, or focus, DMF5 TCR specificity on MART-1 by combining the D26αY and L98βW mutations with additional mutations that weaken the interaction of the TCR with the MHC protein. This is an example of combining positive design with negative design, an approach that has been used in other fields to rationally manipulate binding specificity.[34] In principle, combined positive and negative designs allow for the redistribution of binding free energy in a fashion that forces a greater reliance on favorable TCR interactions with the target peptide, with less tolerance for peptides with characteristics that diverge from the target.[18] This strategy also allows for overall TCR affinity to be maintained within a biologically optimal range.

To identify negative mutations, we examined the crystal structure of the MART-1 decamer in complex with DMF5$_{YW}$. In this structure, Tyr50 of CDR2α is mostly solvent exposed, with the side chain aligned against the HLA-A2 α2 helix in close proximity to the side chains of Glu154, Gln155, and Ala158 (Figure 5A). This geometry is maintained in other structures with the DMF5 TCR or its variants.[32,44] Indeed, Tyr50α regularly interacts with the MHC α2 helix in TCR-pMHC structures, and it has been proposed as an evolutionarily controlled site that contributes to MHC restriction.[45]

We therefore mutated Tyr50α to phenylalanine, valine, and alanine, then measured the impact of these single-mutant variants on DMF5 binding to decameric MART-1/HLA-A2 (Figure 5B). Phenylalanine had a small impact (ΔΔG° of 0.5 kcal/mol), valine an intermediate impact (ΔΔG° of 1.7 kcal/mol), and alanine the largest impact (no binding detected). Based on these results, we combined the
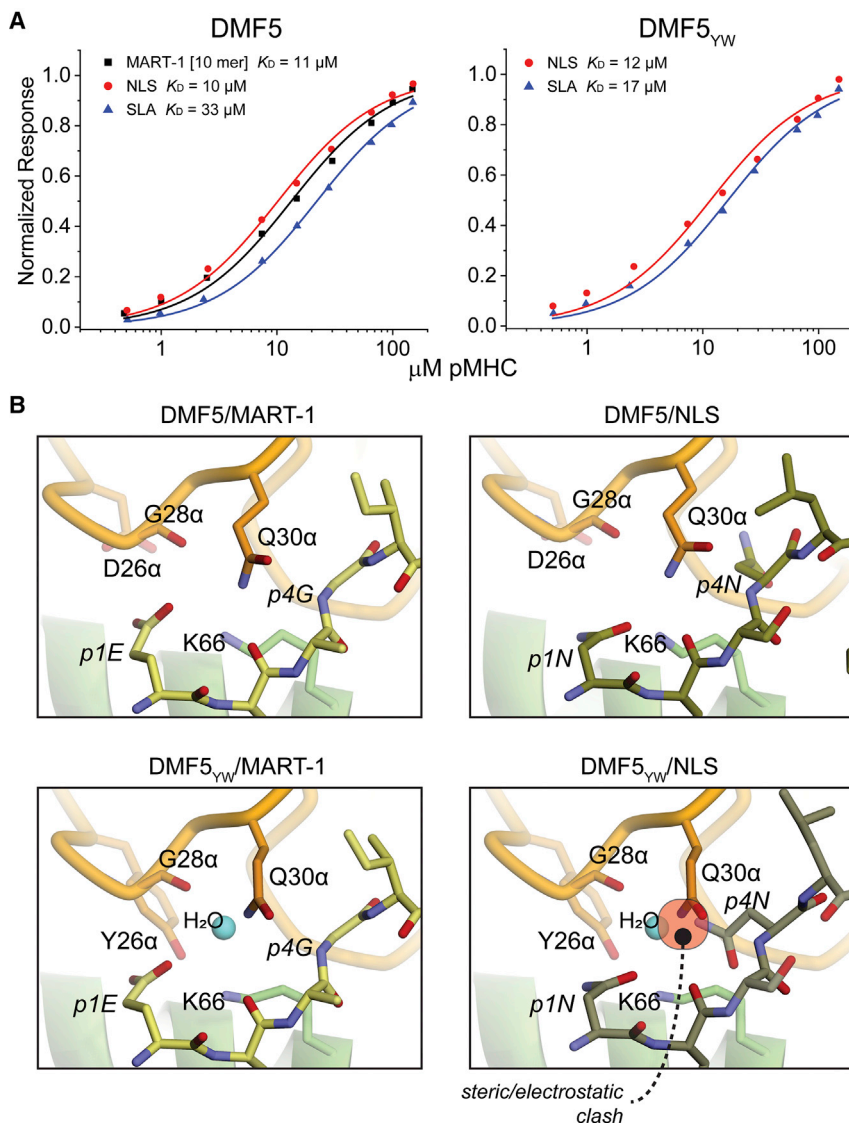
Figure 4. Wild-Type DMF5 and the Highest Affinity DMF5_YW Variant Recognize Decameric Peptides Lacking the MART-1 Core Sequence Similarly

(A) Wild-type DMF5 recognizes the MART-1 decamer and the NLS and SLA peptides with similar affinities (left panel). Surprisingly, affinity toward the NLS and SLA peptides is mostly unchanged with the high-affinity DMF5_YW variant (right panel). (B) Structural basis for cross-recognition. A key difference between the NLS and SLA peptides and the MART-1 homologs is the presence of an asparagine at position 4. Modeling indicates this asparagine can fit within the interface of the wild-type TCR without necessitating significant distortions (top two panels). In the interface with the high-affinity DMF5_YW variant, the asparagine would disrupt a water molecule and require a shift in the position of Gln30 of CDR1α (bottom two panels).

(Figure 3). To confirm that negatively designed mutations at position 50α did not lead to significant structural consequences, we crystallized and determined the structure of DMF5_YW-A bound to the MART-1 decamer presented by HLA-A2 (Table S2; Figure S2). We chose the alanine variant as it was the most perturbative for receptor binding. Overall, the structure with DMF5_YW-A was essentially identical to the structure with DMF5_YW: substituting Tyr50α with alanine did not introduce structural perturbations in the conformation of the CDR2α loop or the HLA-A2 α2 helix or alter how the receptor was positioned over the pMHC (the latter observation is notable given the proposed role for Tyr50α in driving MHC restriction[45]). All common atoms of the DMF5_YW and DMF5_YW-A complexes superimposed with an all-atom RMSD of 1.6 Å. In the interface between CDR2α, the HLA-A2 α2 helix, and the peptide, mutation of Tyr50α to alanine removed the contacts made with Glu154, Gln155, and Ala158 without causing structural distortions (Figure 5C).

Y50αV and Y50αA mutants with the positively designed D26αY/L98βW mutations to generate two MART-1-focused triple mutants, referred to as DMF5_YW-V (D26αY/Y50αV/L98βW) and DMF5_YW-A (D26αY/Y50αA/L98βW). DMF5_YW-V and DMF5_YW-A bound decameric MART-1/HLA-A2 with affinities only slightly weaker than wild-type DMF5 (Figure 5B), with $\Delta\Delta G°$ values of 0.3 kcal/mol for DMF5_YW-V and 0.7 kcal/mol for DMF5_YW-A. Compared to the high-affinity DMF5_YW variant, the loss in binding free energy for introducing the Y50αV and Y50αA mutations was 3.5 kcal/mol and 3.9 kcal/mol, respectively.

Ideally, positive and negative mutations should not have structural impacts that propagate outside of the sites of the mutations. For the positively designed D26αY and L98βW mutations, we previously demonstrated this was the case for DMF5 bound to the MART-1 decamer,[32] and we confirmed it here for the MART-1 nonamer

Positive and Negative Designs Yield Specificity-Tuned DMF5 Variants

We next asked how the MART-1-focused DMF5_YW-A and DMF5_YW-V triple-mutant variants incorporating both positive and negative designs impacted TCR recognition. Experiments measuring intracellular IFN-γ production demonstrated that the two triple mutants retained reactivity toward the MART-1 epitopes and showed reduced recognition of the MART-1 homologs, with the DMF5_YW-A alanine variant appearing slightly less cross-reactive than the DMF5_YW-V valine variant (Figure 6A). Compared to the wild-type TCR, the overall patterns of reactivity of both triple mutants were similar, although again the DMF5_YW-A mutant had a more depressed response against some of the MART-1 homologs than either wild-type DMF5 or DMF5_YW-V

(Figure 6B). We did note that, as observed with the high-affinity DMF5$_{YW}$ variant, the two triple mutants had slightly depressed thermal stabilities compared to the wild-type TCR (Figure S1).

We then asked how DMF5$_{YW-A}$ and DMF5$_{YW-V}$ recognized the peptides that diverge from the MART-1 homology panel. Consistent with the design principles, recognition of the NLS and SLA peptides was sharply reduced compared to both DMF5$_{YW}$ and wild-type DMF5, in agreement with the loss of 3–4 kcal/mol in binding free energy seen when the Y50α mutations were tested with the MART-1 decamer. This resulted in unquantifiable or undetectable binding with the NLS and SLA peptides (Figure 6C; Table S1). Compared to the high-affinity DMF5$_{YW}$ variant, binding toward the MMW peptide was also reduced, yet as DMF5$_{YW}$ bound MMW with nanomolar affinity, mutating Y50αA still resulted in a variant that bound with micromolar affinity (Table S1). Indeed, the ΔΔG° from introducing alanine at Y50α into the DMF5$_{YW}$ was smaller for MMW than MART-1 (2.9 versus 3.9 kcal/mol), resulting in DMF5$_{YW-A}$ binding MMW 2- to 3-fold more tightly than wild-type DMF5 (K_D of 13 versus 35 μM). The smaller ΔΔG° for MMW compared to MART-1 likely results from the mutation increasing solvent exposure around charged amino acids present in the center of the MMW peptide but absent in MART-1.[43]

We next confirmed that reactivity toward the NLS and SLA peptides was eliminated in functional experiments with TCR-transduced T cells. Consistent with the binding data, neither peptide was able to stimulate T cells expressing DMF5$_{YW-V}$ or DMF5$_{YW-A}$ (Figure 6D). This experiment also showed slightly reduced potency toward the MART-1 decamer, consistent with the weaker binding affinity of the DMF5$_{YW-A}$ and DMF5$_{YW-V}$ variants, as shown in Figure 6C (although the weaker TCR stability, as shown in Figure S1A, could also play a role).

Altogether, the data indicate that the combined positive and negative design approach weakened DMF5 cross-reactivity toward the MART-1 homologs and eliminated cross-reactivity with two of the three divergent peptides tested, albeit at the expense of reduced potency toward the target MART-1 antigen. To confirm this overall interpretation, we explored reactivity using a combinatorial peptide library screen, testing the responses of cells transduced with wild-type DMF5, high-affinity DMF5$_{YW}$, or the MART-1-focused DMF5$_{YW-A}$ variant against a decameric library with p2 and p10 anchors fixed at leucine and valine. Although the general results differed from similar experiments on another MART-1-specific TCR in that a clear preference for the MART-1 decamer was not identified,[46] the patterns of reactivity we observed matched those found with our peptide panels and binding experiments: the high-affinity DMF5$_{YW}$ variant showed substantially greater reactivity than wild-type DMF5, and the focused DMF5$_{YW-A}$ variant showed reduced reactivity, albeit with weaker potency (Figure 7A). Estimating the size and overlap of the pools of peptides with stimulatory capacity ≥80% of the maximum observed for each TCR confirmed the more focused nature of the DMF5$_{YW-A}$ variant (Figure 7B).

DISCUSSION

T cell receptor cross-reactivity, or polyspecificity, is fundamental to immunobiology, allowing a fixed-size T cell repertoire to accommodate a much larger universe of potential antigens.[12,13] Yet the ability of a single TCR to engage many different peptide antigens is a challenge for TCR-based immunotherapies due to the potential for off-target toxicity. Efforts to improve TCR specificity by mimicking the antibody affinity maturation process suffer from multiple weaknesses.[18] One is functional, as cells transduced with very high-affinity TCRs can yield weaker potency.[17,28–30] Another is biochemical, as improving TCR affinity can compensate for weak peptide binding to MHC proteins, consequently introducing new peptide reactivities.[47]

Beyond these concerns, the structural architecture of pMHCs poses a significant complication for efforts to improve TCR specificity through affinity enhancement. Peptides presented by MHC proteins typically make up one-third or less of the contacted surface area in TCR-pMHCs.[48,49] The small contact surface of the peptide means there are relatively few peptide features against which affinity can be enhanced. Multiple structurally and chemically related peptides will therefore be compatible with an affinity-enhanced TCR. Due to the high sensitivity of T cells, even a small affinity enhancement toward such peptides could bring them into a range where reactivity is introduced. Our data here confirm this risk, as enhancing the affinity of the DMF5 TCR toward the MART-1 peptides also enhanced affinity and reactivity toward peptides that share the MART-1 core sequence. Thus, even peptide-targeted mutations can still exacerbate cross-reactivity. Lastly, mutations that enhance affinity can potentially enhance recognition of the MHC protein at the expense of the peptide, further negatively impacting peptide specificity. This last possibility is a significant risk when employing random mutagenesis on TCRs, as occurs in the molecular evolution processes such as yeast or phage display.

To add further complexity, due to the sheer number of potential targets a TCR might see, peptide-targeted mutations that avoid the MHC protein and target unique peptide features can have complex, difficult-to-predict outcomes. This is illustrated by our study of peptides recognized by DMF5 that do not share the MART-1 core sequence. These divergent peptides are recognized efficiently by the wild-type TCR, yet, due to competing structural features in the TCR-pMHC interface, the recognition of two of these two divergent peptides is unchanged as affinity toward the MART-1-related peptides is enhanced. Such divergent peptides represent an important class of TCR targets; most will not be typically identified via homology searches, yet divergent peptide cross-recognition is believed to be important in heterologous immunity and T cell memory.[50]

To address the concerns noted above, we explored an approach for engineering TCR specificity, built around the principles of positive and negative structure-guided protein designs. Combining positive and negative designs has been used in other systems to enhance or examine binding specificity,[34,51,52] including bZIP domains and
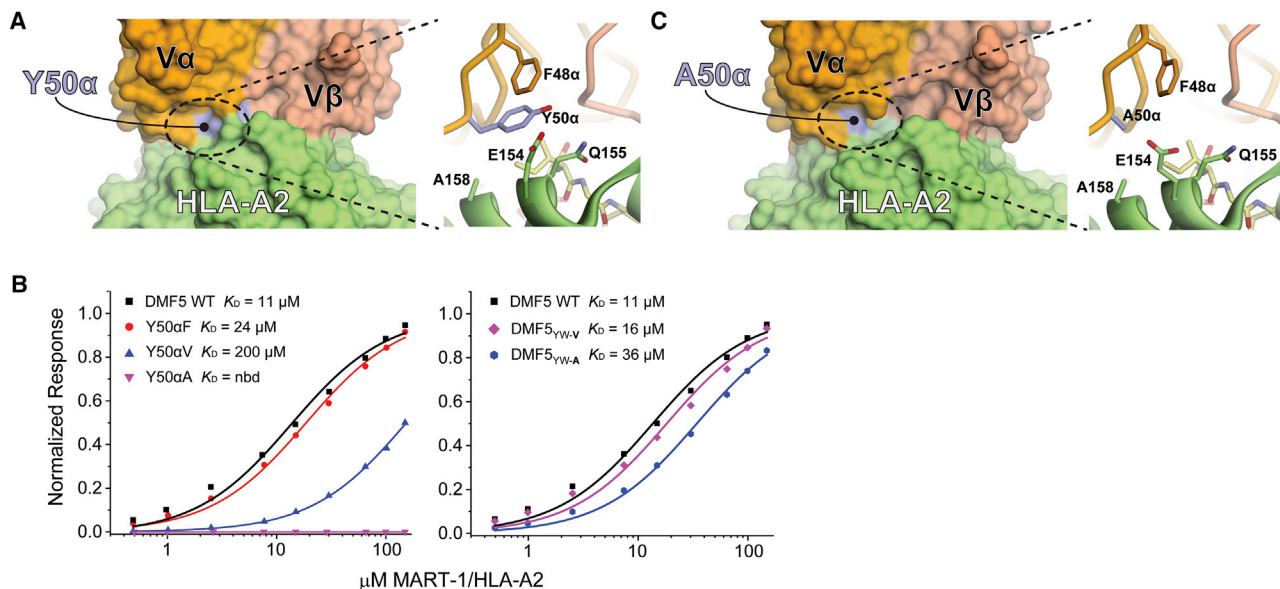
Figure 5. Implementation of a Positive and Negative Design Strategy in the DMF5 TCR

(A) Tyr50 of the DMF5 CDR2α loop interfaces with the HLA-A2 α2 helix, contacting a stretch of amino acids from Gln155 to Ala158. (B) Mutating Tyr50α to phenylalanine, valine, and alanine progressively weakens binding of DMF5 to the MART-1 decamer presented by HLA-A2. nbd, no binding detected (left panel). Combining the Y50αV and Y50αA mutations with the peptide-centric D26αY and L98βW mutations that lead to high-affinity binding, creating the DMF5$_{YW-V}$ and DMF5$_{YW-A}$ triple mutants, returns binding to levels slightly weaker than wild-type (right panel). (C) Mutating Tyr50α to alanine has no gross structural consequences, as shown by the structure of DMF5$_{YW-A}$ bound to the MART-1 decamer presented by HLA-A2.

enzymes.[53,54] Rather than aiming to improve affinity, we aimed to alter the distribution of attractive interactions in the interface (or redistribute binding free energy) in order to reduce the potential for off-target recognition.[18] Our implementation was based on the presumption that affinities that typify TCR recognition of viral antigens (i.e., K_D values in the single- to double-digit micromolar range) are optimal for immunogenicity,[19–21,31] as well as the concern, supported by our findings, that enhancing affinity toward one antigen can enhance affinities toward others, turning non-stimulatory peptides into stimulatory peptides. Positive design involved our previously described, peptide-targeting mutations to the DMF5 TCR.[32] These mutations enhanced binding affinity toward MART-1 up to ∼400-fold, but, as noted, introduced new reactivities. For negative design, we introduced mutations to DMF5 that weaken interactions between the TCR and the HLA-A2 α2 helix.

Compared to the highest affinity DMF5 variants (i.e., variants only possessing the positively designed mutations), the variants incorporating both positive and negative designs appeared superior. Although cross-reactivity toward MART-1 homologs was not eliminated, one of the variants (DMF5$_{YW-A}$) evidenced reduced cross-reactivity, albeit at the expense of weaker potency toward the target MART-1. The inability to more broadly reduce cross-reactivity toward MART-1 homologs indicates that positive design efforts must efficiently target peptide features that distinguish the target from homologs, an important lesson for future developments in TCR design. For TCRs that target MART-1, for example, this could

entail improved targeting of peptide features outside the central core, i.e., near the MART-1 N and C termini.

The potential of the combined positive and negative design strategy was more clearly demonstrated with peptides divergent from MART-1, as cross-reactivity for two of three peptides tested was eliminated with the MART-1-focused variants incorporating positive and negative designs. The ability to engineer out off-target reactivity is a significant achievement, and it provides strong support for using positive and negative designs in TCR engineering. In the case of the MMW peptide where cross-reactivity was not eliminated, the structural and biophysical deconstructions indicated that, like the MART-1 homologs, the positive design mutations enhanced affinity, but, due to structural details in the interface formed with MMW, the impact from negative design was insufficient to overcome the gains from positive design. Lessons from this outcome are that positive and negative design efforts should incorporate as much structural detail as can be made available and that the most optimal mutations are likely to be determined iteratively after assessing reactivity against a broad range of targets in the context of structural information. The use of databases to identify homologs (e.g., Table 1) and screens to identify diverse classes of off-target epitopes will be valuable in identifying targets to study structurally.[55–57]

The fact that the most optimal DMF5 variant generated showed weaker potency toward the target MART-1 antigen is also noteworthy,
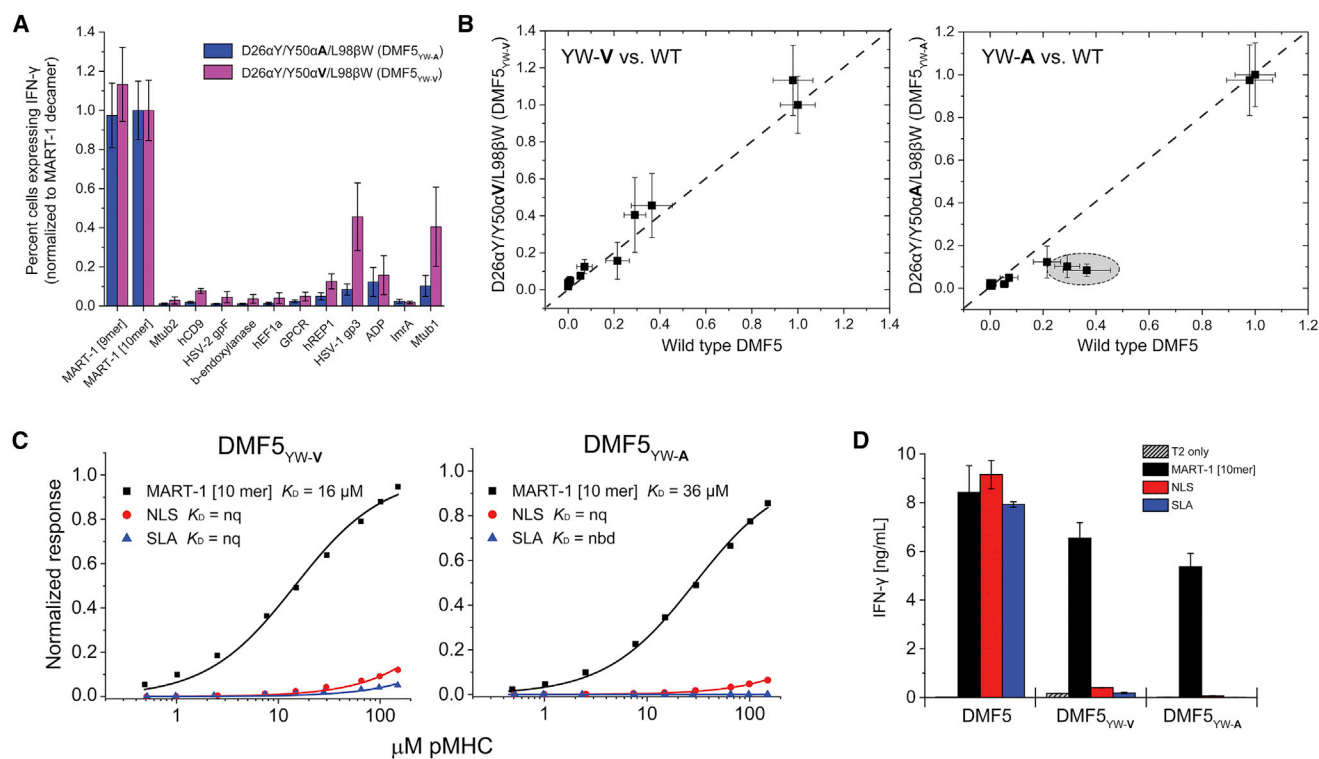
Figure 6. DMF5 Variants Incorporating Positive and Negative Design Principles Show Reduced Cross-Reactivity Compared to High-Affinity and Wild-Type TCR

(A) Percent transduced CD8^{+} T cells expressing intracellular IFN-γ after co-culturing TCR-transduced PBMCs with T2 cells pulsed with the MART-1 peptides and each of the MART-1 homologs in Table 1. Data are averages of six sets of experiments (two independent repeats from three donors), normalized to the values for the MART-1 decamer. Error bars indicate SEM. (B) Direct comparison between the T cell function of wild-type DMF5 and DMF5$_{YW-V}$ and DMF5$_{YW-A}$, using the data from (A) and Figure 2A. Although the patterns of reactivity are similar, the DMF5$_{YW-A}$ mutant is slightly less cross-reactive than the DMF5$_{YW-V}$ mutant (circled region, right panel). (C) DMF5$_{YW-A}$ and DMF5$_{YW-V}$ have substantially reduced binding affinities toward the NLS and SLA peptides presented by HLA-A2, as measured by surface plasmon resonance. nq, binding detectable, but too weak to quantify; nbd, no binding detected. (D) Consistent with the binding experiments, functional recognition of the NLS and SLA peptides is eliminated with DMF5$_{YW-A}$ and DMF5$_{YW-V}$, although potency toward the MART-1 decamer is slightly weaker than with wild-type DMF5. Experiments show IFN-γ secretion when TCR-transduced PBMCs were co-cultured with T2 cells pulsed with peptide. Values are averages of triplicate wells; error bars indicate SDs.

although the low micromolar-binding affinity was still within the range considered optimal for immunogenicity.[20] Reduced potency, whether resulting from slightly weaker TCR binding, weaker TCR stability, or a combination thereof, may be a tradeoff required for enhanced TCR specificity; it could, however, be offset by other technologies designed to increase T cell potency in antigen-independent ways.[58]

In conclusion, having demonstrated the risks of increasing TCR cross-reactivity by enhancing affinity, we tested the potential of advanced structure-based design techniques for improving TCR specificity. Our proof-of-principle study revealed significant promise, although more comprehensive and eventually *in vivo* assessments will be required to fully assess on- and off-target reactivities. In the interim, our data raised design considerations that will need to be addressed for further development and application to other systems. These include the need to identify and carefully evaluate cross-reactive peptides, including structural assessments when possible, as well as the need to iteratively evaluate TCR variants to

identify the most optimal combinations of mutations. Improvements in both structural assessments and the identification of positive and negative mutations will occur with improvements in TCR modeling and design,[59] as well as the intersection between structure-guided protein engineering and advanced protein evolution technologies.[60,61]

MATERIALS AND METHODS

Cells and Media

HEK293GP, PG13, Jurkat, and T2 cell lines were obtained from the American Type Culture Collection. HEK293GP cells were maintained in DMEM supplemented with 10% fetal bovine serum. PG13 cells were maintained in Iscove's DMEM supplemented with 10% fetal bovine serum (FBS). J76 cells are a CD8^{+} Jurkat cell line generated by using a modified SAMEN retroviral vector, as previously described.[9] Jurkat 76 cells, T2 cells, and peripheral blood mononuclear cells (PBMCs) were maintained in RPMI 1640 medium supplemented with 10% FBS. PBMCs were purchased as de-identified apheresis
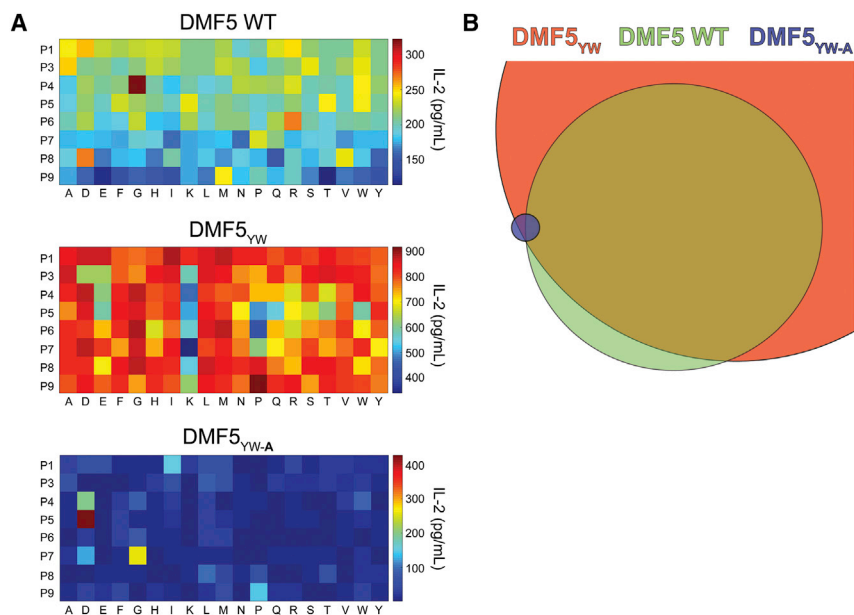
Figure 7. Combinatorial Peptide Library Scans Confirm Outcomes of Positive and Negative Designs

(A) Combinatorial peptide library scans of wild-type DMF5 (top), high-affinity DMF5$_{YW}$ (middle), and MART-1-focused DMF5$_{YW-A}$. For each experiment, TCR-transduced Jurkat 76 cells were incubated with equal numbers of T2 cells pulsed with 152 sub-libraries, where each position of the peptide (excluding primary anchors) was fixed with each of the naturally occurring amino acids (excluding cysteine). Reactivity was assessed by measuring IL-2 release, as indicated by the heatmap scales on the right. Results are the average of three independent experiments with each TCR. (B) Estimate of the relative sizes and sequence overlap of stimulatory peptides from the library for each TCR, accounting for peptides with stimulatory capacity ≥80% of the most potent peptide for each receptor.

products from Key Biologics and isolated using Ficoll-Paque density gradient centrifugation. PBMCs were stimulated prior to transduction with 50 ng/mL anti-CD3 monoclonal antibody (mAb) in RPMI supplemented with 10% FBS, 300 IU/mL interleukin-2 (IL-2), and 100 ng/mL IL-15. T cells were maintained in RPMI supplemented with 10% FBS, 300 IU/mL IL-2, and 100 ng/mL IL-15.

T Cell Transduction

A modified SAMEN retroviral vector was used for the expression of TCR α and β genes in PBMCs and Jurkat 76 cells.[62,63] PG13 cell lines expressing wild-type DMF5 or mutant DMF5 TCRs were used to prepare retroviral supernatants. Generation of stable, high-titer producer PG13 cell lines; preparation of retroviral supernatants; and transduction by spinoculation have been described previously.[64] Transduced T cell cultures were enriched for even and high transgene expression using anti-CD34 mAb-coated immunomagnetic beads.

T Cell Functional Assays

For measurements of intracellular IFN-γ, 3×10^5 transduced T cells were co-cultured with 3×10^5 peptide-pulsed T2 cells in 96-well U-bottom tissue culture plates at 37°C and 5% CO$_2$ for 5 hr; 5.0 ng/mL brefeldin A and 2.0 nM monensin were added at the beginning of co-culture. After 5 hr, cells were stained for 20 min for the following surface markers: anti-CD4-PE/Cy7, anti-CD8-PerCP/Cy5.5, anti-CD3-APC/Cy7, and anti-CD34-PE. Cells were fixed, permeabilized, and stained for intracellular IFN-γ (anti-IFN-γ-Brilliant Violet 421). Data were acquired using an LSRFortessa flow cytometer and analyzed using FlowJo. For measurements of cytokine release, peptide-loaded T2 stimulators were pulsed with 10 μg/mL of the MART-1 peptides or the MART-1 homologs for 2 hr prior to co-culture. 1×10^5 washed and re-suspended effector

T cells and target cells were co-cultured in a 1:1 ratio in triplicate in 96-well U-bottom tissue culture plates in 200 μL medium. Co-cultures were incubated at 37°C and 5% CO$_2$ for 18 hr. The amount of cytokine release was measured in the supernatant by sandwich ELISA using mAbs to IFN-γ.

Combinatorial Peptide Library Scan

A decameric combinatorial peptide library was obtained from Pepscan. The library excluded cysteine and fixed p2 and p10 to leucine and valine, respectively, for a total of 19^8 (approximately 1.7×10^{10}) peptides. The library was composed of 152 sub-libraries in which each position of the peptide, except p2 and p10, was fixed at each amino acid, excluding cysteine, as shown in Figure 7A. The library scan was conducted as previously described,[65,66] pulsing 10^5 T2 cells with 100 μM total peptide concentration of each sub-library for 2 hr at 37°C. Equal numbers of phorbol acetate (PMA)-stimulated (50 ng/mL) Jurkat 76 CD8+ cells transduced with wild-type DMF5, DMF5$_{YW}$, or DMF5$_{YW-A}$ were added and co-cultured for 18–20 hr at 37°C, after which supernatants were harvested and assayed for IL-2 via ELISA. Combinatorial peptide library (CPL) scans were repeated three times with freshly generated cells and the results averaged. For analyzing the CPL data, we calculated the maximum score for each TCR as the sum of the maximum IL-2 released for each sub-library of each peptide position. A list containing all 19^8 peptide sequences in the library was constructed and scored for each TCR as the sum of IL-2 release values observed for the amino acid fixed at that position. These lists were filtered for peptides whose scores were ≥80% of the maximum score for that TCR. Data processing and analysis utilized custom Python and shell scripts.

Recombinant Proteins and Peptides

Soluble constructs of DMF5 TCRs and HLA-A2 were expressed and refolded as previously described.[32,67] Briefly, the TCR α and β chains, the HLA-A2 heavy chain, and β$_2$-microglobulin (β$_2$m)

were expressed in *Escherichia coli* as inclusion bodies, then isolated and denatured in 8M urea. Equimolar amounts of TCR α and β chains were diluted in refolding buffer (50 mM Tris [pH 8], 2.5 M urea, 2 mM EDTA, 9.6 mM cysteamine, 3.7 mM cystamine, and 0.2 mM PMSF). For MHC, 3:1 molar ratios of β_2m to HLA-A2 were diluted in MHC refolding buffer (100 mM Tris [pH 8], 400 mM L-arginine, 2 mM EDTA, 6.3 mM cysteamine, 3.7 mM cystamine, and 0.2 mM PMSF) in the presence of excess peptide. For refolding, TCR and pMHCs were incubated overnight at 4°C. Assembled TCR and pMHC were desalted by dialysis at 4°C and room temperature, respectively. Samples were purified by anion exchange followed by size-exclusion chromatography. Protein concentrations were measured spectroscopically at 280 nm. DMF5 mutations were performed by PCR mutagenesis and confirmed by sequencing. Peptides for functional assays were obtained from Synthetic Biomolecules, purified to 95% purity, and stored at 10 μg/mL in 100% DMSO at −80°C. Peptides for structural and biophysical studies were purchased from AAPPTec and Chi Scientific, purified to 90% purity, and stored at 30 mM in 100% DMSO at −20°C.

Binding Assays

SPR experiments were performed with a Biacore T200 instrument. The TCR was immobilized to CM-5 sensor chips via amine coupling, and pMHC was injected as analyte in all experiments. Samples were dialyzed in HBS-EP buffer (10 mM HEPES [pH 7.4], 150 mM NaCl, 3 mM EDTA, and 0.005% surfactant P-20), then degassed for at least 15 min prior to use. Most experiments used a steady-state-binding assay, in which TCRs were coupled to the chips at 1,500–2,000 response units. pMHC injections covered a concentration range of 0.5–150 μM at a flow rate of 5 μL/min at 25°C. To extend the range and accuracy of measurements, multiple steady-state datasets were globally fit using a 1:1 Langmuir binding model with BIAevaluation 4.1, as described previously.[37,38] Measurements of TCR binding to the MMW/HLA-A2 complex were performed using a kinetic titration assay at 25°C,[68] with chip densities near 150 resonance units (RU) for DMF5$_{YW}$ and 500 RU for DMF5$_{YW-A}$. pMHC concentrations ranged from 32 to 500 nM for DMF5$_{YW}$ and 1 to 16 μM for DMF5$_{YW-A}$. Kinetic titrations used a flow rate of 100 μL/min.

Thermal Stability Measurements

TCR thermal stability was measured using differential scanning fluorimetry using an Applied Biosystems StepOnePlus RT-PCR instrument. The excitation and emission wavelengths were set to 587 and 607 nm, respectively. Samples volumes of 20 μL were aliquoted into a 96-well plate at a final concentration of 10 μM protein with 10× SYPRO orange dye. pMHC thermal stability was measured using a NanoTemper Prometheus instrument collecting scattering data, with a 50- to 100-μM protein concentration. TCR and pMHC stabilities were measured in 10 mM HEPES (pH 7.4), 150 mM NaCl, 3 mM EDTA, and 0.005% surfactant P20. Temperatures spanned 25°C–95°C with an increment of 1°C/min. TCR and pMHC thermal stability data were analyzed using OriginPro 7 or 9.

T_m values were obtained by computing the derivative of the melting curve and fitting to a bi-Gaussian function with a sigmoidal baseline, as previously described.[69]

Crystallization and Structure Determination

Crystals of the complex of DMF5$_{YW}$ bound to nonameric MART-1/HLA-A2 were grown in 12% PEG 6000 and 200 mM MgCl$_2$, buffered in 100 mM Tris (pH 7.5) at 25°C. Crystals of the complex of DMF5$_{YW-A}$ bound to decameric MART-1/HLA-A2 were grown in 12% PEG 3350 and 250 mM MgCl$_2$, buffered in 100 mM HEPES (pH 8) at 25°C. Diffraction data were collected at the 22ID (SER-CAT; DMF5$_{YW}$ complex) and 24ID-C (NE-CAT; DMF5$_{YW-A}$ complex) beamlines at the Advanced Photon Source at Argonne National Laboratories. Data integration and scaling were performed using XDS and AIMLESS, respectively. Complexes were solved by Phaser-molecular replacement using PHENIX[70] and PDB: 4L3E (DMF5$_{YW}$ complex) or PDB: 3QDG (DMF5$_{YW-A}$ complex) as the reference models with CDR loops and peptides removed. For DMF5$_{YW}$ bound to nonameric MART-1/HLA-A2, model building was carried out using PHENIX AutoBuild followed by several rounds of restrained refinement using PHENIX Refine. For DMF5$_{YW-A}$ bound to the decameric MART-1/HLA-A2 complex, AutoBuild was used for model building, followed by successive restrained refinement using PHENIX Refine and Rosetta Refinement. For both complexes, translation/libration/screw parameters were included during refinement, with the complexes split into eight domains (each TCR chain split into variable and constant domains and the pMHC molecule split among β_2-microglobulin, the α3 domain, the peptide-binding groove, and the peptide). Evaluation of models and fitting to maps were performed using Coot.[71] The template structure check in MolProbity was used to evaluate the structures during and after refinement.[72] Atomic positioning was verified by simulated annealing OMIT maps calculated in PHENIX.

Structural Modeling

Structural modeling of TCR-peptide/HLA-A2 complexes was performed using Rosetta with the Talaris2013 score function and the PyRosetta interface.[73,74] Using the relax protocol, five cycles of backbone minimization and rotamer optimization brought the PDB template structures (PDB: 3QDG for the wild-type and PDB: 4L3E for the high-affinity structure) to a local energy minimum. Following minimization, the desired peptide sequence was computationally introduced, followed by 50 Monte Carlo-based simulated annealing steps for the peptide backbone. The lowest energy structures were retained for further analysis. Energies of the final models were ranked relative to each other using a previously published score function parameterized for quantifying the strength of protein-protein interactions.[75] The SLA peptide was identified by considering scores of substituted amino acids after modeling in the NLS peptide, as described previously.[59]

SUPPLEMENTAL INFORMATION

Supplemental Information includes two figures and two tables and can be found with this article online at https://doi.org/10.1016/j.ymthe.2018.12.010.

AUTHOR CONTRIBUTIONS

CONFLICTS OF INTEREST

B.M.B. is on the board of a University startup aimed at modulating immune specificity.

ACKNOWLEDGMENTS

REFERENCES

1. Johnson, L.A., Morgan, R.A., Dudley, M.E., Cassard, L., Yang, J.C., Hughes, M.S., Kammula, U.S., Royal, R.E., Sherry, R.M., Wunderlich, J.R., et al. (2009). Gene therapy with human and mouse T-cell receptors mediates cancer regression and targets normal tissues expressing cognate antigen. Blood 114, 535–546.

2. Duval, L., Schmidt, H., Kaltoft, K., Fode, K., Jensen, J.J., Sorensen, S.M., Nishimura, M.I., and von der Maase, H. (2006). Adoptive transfer of allogeneic cytotoxic T lymphocytes equipped with a HLA-A2 restricted MART-1 T-cell receptor: a phase I trial in metastatic melanoma. Clin. Cancer Res. 12, 1229–1236.

3. Morgan, R.A., Dudley, M.E., Wunderlich, J.R., Hughes, M.S., Yang, J.C., Sherry, R.M., Royal, R.E., Topalian, S.L., Kammula, U.S., Restifo, N.P., et al. (2006). Cancer regression in patients after transfer of genetically engineered lymphocytes. Science 314, 126–129.

4. Robbins, P.F., Morgan, R.A., Feldman, S.A., Yang, J.C., Sherry, R.M., Dudley, M.E., Wunderlich, J.R., Nahvi, A.V., Helman, L.J., Mackall, C.L., et al. (2011). Tumor regression in patients with metastatic synovial cell sarcoma and melanoma using genetically engineered lymphocytes reactive with NY-ESO-1. J. Clin. Oncol. 29, 917–924.

5. Moore, T., Wagner, C.R., Scurti, G.M., Hutchens, K.A., Godellas, C., Clark, A.L., Kolawole, E.M., Hellman, L.M., Singh, N.K., Huyke, F.A., et al. (2018). Clinical and immunologic evaluation of three metastatic melanoma patients treated with autologous melanoma-reactive TCR-transduced T cells. Cancer Immunol. Immunother. 67, 311–325.

6. Johnson, L.A., and June, C.H. (2017). Driving gene-engineered T cell immunotherapy of cancer. Cell Res. 27, 38–58.

7. Parida, S.K., Poiret, T., Zhenjiang, L., Meng, Q., Heyckendorf, J., Lange, C., Ambati, A.S., Rao, M.V., Valentini, D., Ferrara, G., et al. (2015). T-Cell Therapy: Options for Infectious Diseases. Clin. Infect. Dis. 61 (61, Suppl 3), S217–S224.

8. Leibman, R.S., and Riley, J.L. (2015). Engineering T Cells to Functionally Cure HIV-1 Infection. Mol. Ther. 23, 1149–1159.

9. Spear, T.T., Riley, T.P., Lyons, G.E., Callender, G.G., Roszkowski, J.J., Wang, Y., Simms, P.E., Scurti, G.M., Foley, K.C., Murray, D.C., et al. (2016). Hepatitis C virus-cross-reactive TCR gene-modified T cells: a model for immunotherapy against diseases with genomic instability. J. Leukoc. Biol. 100, 545–557.

10. Linette, G.P., Stadtmauer, E.A., Maus, M.V., Rapoport, A.P., Levine, B.L., Emery, L., Litzky, L., Bagg, A., Carreno, B.M., Cimino, P.J., et al. (2013). Cardiovascular toxicity and titin cross-reactivity of affinity-enhanced T cells in myeloma and melanoma. Blood 122, 863–871.

11. Wucherpfennig, K.W., Allen, P.M., Celada, F., Cohen, I.R., De Boer, R., Garcia, K.C., Goldstein, B., Greenspan, R., Hafler, D., Hodgkin, P., et al. (2007). Polyspecificity of T cell and B cell receptor recognition. Semin. Immunol. 19, 216–224.

12. Mason, D. (1998). A very high level of crossreactivity is an essential feature of the T-cell receptor. Immunol. Today 19, 395–404.

13. Sewell, A.K. (2012). Why must T cells be cross-reactive? Nat. Rev. Immunol. 12, 669–677.

14. Gee, M.H., Sibener, L.V., Birnbaum, M.E., Jude, K.M., Yang, X., Fernandes, R.A., Mendoza, J.L., Glassman, C.R., and Garcia, K.C. (2018). Stress-testing the relationship between T cell receptor/peptide-MHC affinity and cross-reactivity using peptide velcro. Proc. Natl. Acad. Sci. USA 115, E7369–E7378.

15. Holler, P.D., Chlewicki, L.K., and Kranz, D.M. (2003). TCRs with high affinity for foreign pMHC show self-reactivity. Nat. Immunol. 4, 55–62.

16. Zhao, Y., Bennett, A.D., Zheng, Z., Wang, Q.J., Robbins, P.F., Yu, L.Y.L., Li, Y., Molloy, P.E., Dunn, S.M., Jakobsen, B.K., et al. (2007). High-affinity TCRs generated by phage display provide CD4+ T cells with the ability to recognize and kill tumor cell lines. J. Immunol. 179, 5845–5854.

17. Tan, M.P., Gerry, A.B., Brewer, J.E., Melchiori, L., Bridgeman, J.S., Bennett, A.D., Pumphrey, N.J., Jakobsen, B.K., Price, D.A., Ladell, K., and Sewell, A.K. (2015). T cell receptor binding affinity governs the functional profile of cancer-specific CD8+ T cells. Clin. Exp. Immunol. 180, 255–270.

18. Riley, T.P., and Baker, B.M. (2018). The intersection of affinity and specificity in the development and optimization of T cell receptor based therapeutics. Semin. Cell Dev. Biol. 84, 30–41.

19. Stone, J.D., and Kranz, D.M. (2013). Role of T cell receptor affinity in the efficacy and specificity of adoptive T cell therapies. Front. Immunol. 4, 244.

20. Hebeisen, M., Oberle, S.G., Presotto, D., Speiser, D.E., Zehn, D., and Rufer, N. (2013). Molecular insights for optimizing T cell receptor specificity against cancer. Front. Immunol. 4, 154.

21. Slansky, J.E., and Jordan, K.R. (2010). The Goldilocks model for TCR-too much attraction might not be best for vaccine design. PLoS Biol. 8, e1000482.

22. Malecek, K., Grigoryan, A., Zhong, S., Gu, W.J., Johnson, L.A., Rosenberg, S.A., Cardozo, T., and Krogsgaard, M. (2014). Specific increase in potency via structure-based design of a TCR. J. Immunol. 193, 2587–2599.

23. Varela-Rohena, A., Molloy, P.E., Dunn, S.M., Li, Y., Suhoski, M.M., Carroll, R.G., Milicic, A., Mahon, T., Sutton, D.H., Laugel, B., et al. (2008). Control of HIV-1 immune escape by CD8 T cells expressing enhanced T-cell receptor. Nat. Med. 14, 1390–1395.

24. Irving, M., Zoete, V., Hebeisen, M., Schmid, D., Baumgartner, P., Guillaume, P., Romero, P., Speiser, D., Luescher, I., Rufer, N., and Michielin, O. (2012). Interplay between T cell receptor binding kinetics and the level of cognate peptide presented by major histocompatibility complexes governs CD8+ T cell responsiveness. J. Biol. Chem. 287, 23068–23078.

25. Holler, P.D., Lim, A.R., Cho, B.K., Rund, L.A., and Kranz, D.M. (2001). CD8(-) T cell transfectants that express a high affinity T cell receptor exhibit enhanced peptide-dependent activation. J. Exp. Med. 194, 1043–1052.

26. Robbins, P.F., Li, Y.F., El-Gamil, M., Zhao, Y., Wargo, J.A., Zheng, Z., Xu, H., Morgan, R.A., Feldman, S.A., Johnson, L.A., et al. (2008). Single and dual amino acid substitutions in TCR CDRs can enhance antigen-specific T cell functions. J. Immunol. 180, 6116–6131.

27. Schmitt, T.M., Aggen, D.H., Stromnes, I.M., Dossett, M.L., Richman, S.A., Kranz, D.M., and Greenberg, P.D. (2013). Enhanced-affinity murine T-cell receptors for tumor/self-antigens can be safe in gene therapy despite surpassing the threshold for thymic selection. Blood 122, 348–356.

28. Hebeisen, M., Baitsch, L., Presotto, D., Baumgaertner, P., Romero, P., Michielin, O., Speiser, D.E., and Rufer, N. (2013). SHP-1 phosphatase activity counteracts increased T cell receptor affinity. J. Clin. Invest. 123, 1044–1056.

29. Engels, B., Chervin, A.S., Sant, A.J., Kranz, D.M., and Schreiber, H. (2012). Long-term persistence of CD4(+) but rapid disappearance of CD8(+) T cells expressing an MHC class I-restricted TCR of nanomolar affinity. Mol. Ther. 20, 652–660.

30. Corse, E., Gottschalk, R.A., Krogsgaard, M., and Allison, J.P. (2010). Attenuated T cell responses to a high-potency ligand in vivo. PLoS Biol. 8, e1000481.

31. Zhong, S., Malecek, K., Johnson, L.A., Yu, Z., Vega-Saenz de Miera, E., Darvishian, F., McGary, K., Huang, K., Boyer, J., Corse, E., et al. (2013). T-cell receptor affinity and avidity defines antitumor response and autoimmunity in T-cell immunotherapy. Proc. Natl. Acad. Sci. USA 110, 6973–6978.

32. Pierce, B.G., Hellman, L.M., Hossain, M., Singh, N.K., Vander Kooi, C.W., Weng, Z., and Baker, B.M. (2014). Computational design of the affinity and specificity of a therapeutic T cell receptor. PLoS Comput. Biol. 10, e1003478.

33. Johnson, L.A., Heemskerk, B., Powell, D.J., Jr., Cohen, C.J., Morgan, R.A., Dudley, M.E., Robbins, P.F., and Rosenberg, S.A. (2006). Gene transfer of tumor-reactive TCR confers both high avidity and tumor reactivity to nonreactive peripheral blood mononuclear cells and tumor-infiltrating lymphocytes. J. Immunol. 177, 6548–6559.

34. Karanicolas, J., and Kuhlman, B. (2009). Computational design of affinity and specificity at protein-protein interfaces. Curr. Opin. Struct. Biol. 19, 458–463.

35. Hawse, W.F., Champion, M.M., Joyce, M.V., Hellman, L.M., Hossain, M., Ryan, V., Pierce, B.G., Weng, Z., and Baker, B.M. (2012). Cutting edge: Evidence for a dynamically driven T cell signaling mechanism. J. Immunol. 188, 5819–5823.

36. Loftus, D.J., Castelli, C., Clay, T.M., Squarcina, P., Marincola, F.M., Nishimura, M.I., Parmiani, G., Appella, E., and Rivoltini, L. (1996). Identification of epitope mimics recognized by CTL reactive to the melanoma/melanocyte-derived peptide MART-1(27-35). J. Exp. Med. 184, 647–657.

37. Blevins, S.J., and Baker, B.M. (2017). Using Global Analysis to Extend the Accuracy and Precision of Binding Measurements with T cell Receptors and Their Peptide/MHC Ligands. Front. Mol. Biosci. 4, 2.

38. Piepenbrink, K.H., Gloor, B.E., Armstrong, K.M., and Baker, B.M. (2009). Methods for quantifying T cell receptor binding affinities and thermodynamics. Methods Enzymol. 466, 359–381.

39. Das, R., and Baker, D. (2008). Macromolecular modeling with rosetta. Annu. Rev. Biochem. 77, 363–382.

40. Singh, N.K., Riley, T.P., Baker, S.C.B., Borrman, T., Weng, Z., and Baker, B.M. (2017). Emerging Concepts in TCR Specificity: Rationalizing and (Maybe) Predicting Outcomes. J. Immunol. 199, 2203–2213.

41. Antunes, D.A., Rigo, M.M., Freitas, M.V., Mendes, M.F.A., Sinigaglia, M., Lizée, G., Kavraki, L.E., Selin, L.K., Cornberg, M., and Vieira, G.F. (2017). Interpreting T-Cell Cross-reactivity through Structure: Implications for TCR-Based Cancer Immunotherapy. Front. Immunol. 8, 1210.

42. Gee, M.H., Han, A., Lofgren, S.M., Beausang, J.F., Mendoza, J.L., Birnbaum, M.E., Bethune, M.T., Fischer, S., Yang, X., Gomez-Eerland, R., et al. (2018). Antigen Identification for Orphan T Cell Receptors Expressed on Tumor-Infiltrating Lymphocytes. Cell 172, 549–563.e16.

43. Riley, T.P., Hellman, L.M., Gee, M.H., Mendoza, J.L., Alonso, J.A., Foley, K.C., Nishimura, M.I., Vander Kooi, C.W., Garcia, K.C., and Baker, B.M. (2018). T cell receptor cross-reactivity expanded by dramatic peptide-MHC adaptability. Nat. Chem. Biol. 14, 934–942.

44. Borbulevych, O.Y., Santhanagopolan, S.M., Hossain, M., and Baker, B.M. (2011). TCRs used in cancer gene therapy cross-react with MART-1/Melan-A tumor antigens via distinct mechanisms. J. Immunol. 187, 2453–2463.

45. Marrack, P., Scott-Browne, J.P., Dai, S., Gapin, L., and Kappler, J.W. (2008). Evolutionarily conserved amino acids that control TCR-MHC interaction. Annu. Rev. Immunol. 26, 171–203.

46. Ekeruche-Makinde, J., Clement, M., Cole, D.K., Edwards, E.S.J., Ladell, K., Miles, J.J., Matthews, K.K., Fuller, A., Lloyd, K.A., Madura, F., et al. (2012). T-cell receptor-optimized peptide skewing of the T-cell repertoire can enhance antigen targeting. J. Biol. Chem. 287, 37269–37281.

47. Bowerman, N.A., Crofts, T.S., Chlewicki, L., Do, P., Baker, B.M., Christopher Garcia, K., and Kranz, D.M. (2009). Engineering the binding properties of the T cell receptor:peptide:MHC ternary complex that governs T cell activity. Mol. Immunol. 46, 3000–3008.

48. Rossjohn, J., Gras, S., Miles, J.J., Turner, S.J., Godfrey, D.I., and McCluskey, J. (2015). T cell antigen receptor recognition of antigen-presenting molecules. Annu. Rev. Immunol. 33, 169–200.

49. Rudolph, M.G., Stanfield, R.L., and Wilson, I.A. (2006). How TCRs bind MHCs, peptides, and coreceptors. Annu. Rev. Immunol. 24, 419–466.

50. Brehm, M.A., Pinto, A.K., Daniels, K.A., Schneck, J.P., Welsh, R.M., and Selin, L.K. (2002). T cell immunodominance and maintenance of memory regulated by unexpectedly cross-reactive pathogens. Nat. Immunol. 3, 627–634.

51. Havranek, J.J., and Harbury, P.B. (2003). Automated design of specificity in molecular recognition. Nat. Struct. Biol. 10, 45–52.

52. Schreiber, G., and Keating, A.E. (2011). Protein binding specificity versus promiscuity. Curr. Opin. Struct. Biol. 21, 50–61.

53. Grigoryan, G., Reinke, A.W., and Keating, A.E. (2009). Design of protein-interaction specificity gives selective bZIP-binding peptides. Nature 458, 859–864.

54. Frey, K.M., Georgiev, I., Donald, B.R., and Anderson, A.C. (2010). Predicting resistance mutations using protein design algorithms. Proc. Natl. Acad. Sci. USA 107, 13707–13712.

55. Birnbaum, M.E., Mendoza, J.L., Sethi, D.K., Dong, S., Glanville, J., Dobbins, J., Ozkan, E., Davis, M.M., Wucherpfennig, K.W., and Garcia, K.C. (2014). Deconstructing the peptide-MHC specificity of T cell recognition. Cell 157, 1073–1087.

56. Adams, J.J., Narayanan, S., Birnbaum, M.E., Sidhu, S.S., Blevins, S.J., Gee, M.H., Sibener, L.V., Baker, B.M., Kranz, D.M., and Garcia, K.C. (2016). Structural interplay between germline interactions and adaptive recognition determines the bandwidth of TCR-peptide-MHC cross-reactivity. Nat. Immunol. 17, 87–94.

57. Wooldridge, L., Ekeruche-Makinde, J., van den Berg, H.A., Skowera, A., Miles, J.J., Tan, M.P., Dolton, G., Clement, M., Llewellyn-Lacey, S., Price, D.A., et al. (2012). A single autoimmune T cell receptor recognizes more than a million different peptides. J. Biol. Chem. 287, 1168–1177.

58. Kaczanowska, S., Joseph, A.M., Guo, J., Tsai, A.K., Lasola, J.J., Younger, K., Zhang, Y., Gonzales, C.V., and Davila, E. (2017). A Synthetic CD8α:MyD88 Coreceptor Enhances CD8+ T-cell Responses to Weakly Immunogenic and Lowly Expressed Tumor Antigens. Cancer Res. 77, 7049–7058.

59. Riley, T.P., Ayres, C.M., Hellman, L.M., Singh, N.K., Cosiano, M., Cimons, J.M., Anderson, M.J., Piepenbrink, K.H., Pierce, B.G., Weng, Z., and Baker, B.M. (2016). A generalized framework for computational design and mutational scanning of T-cell receptor binding interfaces. Protein Eng. Des. Sel. 29, 595–606.

60. Harris, D.T., Wang, N., Riley, T.P., Anderson, S.D., Singh, N.K., Procko, E., Baker, B.M., and Kranz, D.M. (2016). Deep Mutational Scans as a Guide to Engineering High Affinity T Cell Receptor Interactions with Peptide-bound Major Histocompatibility Complex. J. Biol. Chem. 291, 24566–24578.

61. Harris, D.T., Singh, N.K., Cai, Q., Smith, S.N., Vander Kooi, C., Procko, E., Kranz, D.M., and Baker, B.M. (2016). An Engineered Switch in T Cell Receptor Specificity Leads to an Unusual but Functional Binding Geometry. Structure 24, 1142–1154.

62. Callender, G.G., Rosen, H.R., Roszkowski, J.J., Lyons, G.E., Li, M., Moore, T., Brasic, N., McKee, M.D., and Nishimura, M.I. (2006). Identification of a hepatitis C virus-reactive T cell receptor that does not require CD8 for target cell recognition. Hepatology 43, 973–981.

63. Lyons, G.E., Moore, T., Brasic, N., Li, M., Roszkowski, J.J., and Nishimura, M.I. (2006). Influence of human CD8 on antigen recognition by T-cell receptor-transduced cells. Cancer Res. 66, 11455–11461.

64. Foley, K.C., Spear, T.T., Murray, D.C., Nagato, K., Garrett-Mayer, E., and Nishimura, M.I. (2017). HCV T Cell Receptor Chain Modifications to Enhance Expression, Pairing, and Antigen Recognition in T Cells for Adoptive Transfer. Mol. Ther. Oncolytics 5, 105–115.

65. Cole, D.K., Bulek, A.M., Dolton, G., Schauenberg, A.J., Szomolay, B., Rittase, W., Trimby, A., Jothikumar, P., Fuller, A., Skowera, A., et al. (2016). Hotspot autoimmune T cell receptor binding underlies pathogen and insulin peptide cross-reactivity. J. Clin. Invest. 126, 2191–2204.

66. Wooldridge, L., Laugel, B., Ekeruche, J., Clement, M., van den Berg, H.A., Price, D.A., and Sewell, A.K. (2010). CD8 controls T cell cross-reactivity. J. Immunol. 185, 4625–4632.

67. Davis-Harrison, R.L., Armstrong, K.M., and Baker, B.M. (2005). Two different T cell receptors use different thermodynamic strategies to recognize the same peptide/MHC ligand. J. Mol. Biol. 346, 533–550.

68. Karlsson, R., Katsamba, P.S., Nordin, H., Pol, E., and Myszka, D.G. (2006). Analyzing a kinetic titration series using affinity biosensors. Anal. Biochem. 349, 136–147.

69. Hellman, L.M., Yin, L., Wang, Y., Blevins, S.J., Riley, T.P., Belden, O.S., Spear, T.T., Nishimura, M.I., Stern, L.J., and Baker, B.M. (2016). Differential scanning fluorimetry

based assessments of the thermal and kinetic stability of peptide-MHC complexes. J. Immunol. Methods *432*, 95–101.

70. Adams, P.D., Afonine, P.V., Bunkóczi, G., Chen, V.B., Echols, N., Headd, J.J., Hung, L.W., Jain, S., Kapral, G.J., Grosse Kunstleve, R.W., et al. (2011). The Phenix software for automated determination of macromolecular structures. Methods *55*, 94–106.

71. Emsley, P., and Cowtan, K. (2004). Coot: model-building tools for molecular graphics. Acta Crystallogr. D Biol. Crystallogr. *60*, 2126–2132.

72. Chen, V.B., Arendall, W.B., 3rd, Headd, J.J., Keedy, D.A., Immormino, R.M., Kapral, G.J., Murray, L.W., Richardson, J.S., and Richardson, D.C. (2010). MolProbity: all-atom structure validation for macromolecular crystallography. Acta Crystallogr. D Biol. Crystallogr. *66*, 12–21.

73. Kaufmann, K.W., Lemmon, G.H., Deluca, S.L., Sheehan, J.H., and Meiler, J. (2010). Practically useful: what the Rosetta protein modeling suite can do for you. Biochemistry *49*, 2987–2998.

74. Chaudhury, S., Lyskov, S., and Gray, J.J. (2010). PyRosetta: a script-based interface for implementing molecular modeling algorithms using Rosetta. Bioinformatics *26*, 689–691.

75. Kortemme, T., and Baker, D. (2002). A simple physical model for binding energy hot spots in protein-protein complexes. Proc. Natl. Acad. Sci. USA *99*, 14116–14121.

76. Crooks, G.E., Hon, G., Chandonia, J.-M., and Brenner, S.E. (2004). WebLogo: a sequence logo generator. Genome Res. *14*, 1188–1190.